(11) Gelles, R.; Frank, C. W. *Macromolecules* **1982**, *15*, 741.
(12) Winnik, M. in ref 8b.
(13) Torkelson, J. M.; Lipsky, S.; Tirrell, M. *Macromolecules* **1981**, *14*, 1603.
(14) Lindsell, W. E.; Robertson, F. C.; Soutar, I. *Eur. Polym. J.* **1981**, *17*, 203.
(15) Sanchez-Renamayor, C.; Radic, D.; Gargallo, L.; Pierola, I. F. *Polym. Prep. (Am. Chem. Soc., Div. Polym. Chem.)* **1987**, *28*, 195.
(16) Frank, C. W.; Gelles, R. in ref 8b, 564.
(17) Yoon, D. Y.; Sundararajan, P. R.; Flory, P. J. *Macromolecules* **1975**, *8*, 776.
(18) Mark, J. E.; Ko, J. H. *J. Polym. Sci., Polym. Phys. Ed.* **1975**, *13*, 2221.
(19) Rubio, A. M.; Freire, J. J. *Macromolecules* **1982**, *15*, 1411.
(20) Freire, J. J.; Rubio, A. M. *J. Chem. Phys.* **1984**, *81*, 2112.
(21) Rubio, A. M.; Freire, J. J. *Macromolecules* **1989**, *22*, 333.
(22) Reynders, P.; Dreeskamp, H.; Kuhnle, W.; Zachariasse, A. *J. Phys. Chem.* **1987**, *91*, 3982.
(23) Blonski, S.; Sienicki, K. *Macromolecules* **1986**, *19*, 2936.
(24) Scott, D. W.; Messerly, J. F.; Todd, S. S.; Guthrie, G. B.; Hossenlopp, I. A.; Moore, R. T.; Osborn, A.; Berg, W. T.; McCollough, J. P. *J. Phys. Chem.* **1961**, *65*, 1320.
(25) Ishii, T.; Handa, T.; Matsunaga, J. *Macromolecules* **1978**, *11*, 40.
(26) Abuín, E.; Lissi, E.; Gargallo, L.; Radic, D. *Eur. Polym. J.* **1984**, *20*, 105.
(27) Ishii, T.; Handa, T.; Matsunaga, S. *Makromol. Chem.* **1977**, *178*, 2351.
(28) McCallum, J. R. In *Photophysics of Polymers*; Hoyle, C. E., Torkelson, J. M., Eds.; ACS Symposium *Series* 358; American Chemical Society: Washington, DC, 1987.
(29) (a) Bokobza, L.; Monnerie, L. *Polymer* **1981**, *22*, 235. (b) Fox, R. B.; Price, T. R.; Cozzens, R. F.; McDonald, J. R. *J. Chem. Phys.* **1972**, *57*, 534.
(30) Wu, S. K.; Jiang, Y. C.; Rabek, J. F. *Polym. Bull.* **1980**, *3*, 319.
(31) Phillips, D.; Roberts, A. J.; Rumbles, G.; Soutar, I. *Macromolecules* **1983**, *16*, 1597.
(32) Vala, M. T., Jr.; Haebig, J.; Rice, S. A. *J. Chem. Phys.* **1965**, *43*, 886.
(33) Ghiggino, K. P.; Wright, R. D.; Phillips, D. *J. Polym. Sci., Polym. Phys. Ed.* **1978**, *16*, 1499.
(34) Frank, C. W.; Harrah, L. A. *J. Chem. Phys.* **1974**, *61*, 1526.
(35) In the m(tt) equilibrium conformers, neighboring rings may not be perfectly parallel (ref 17 for the case of PS), and therefore, a reorientation of phenyl groups may also be needed for excimer formation.
(36) De Schryver, F. C.; Moens, L.; Van der Auweraer, M.; Boens, N.; Monnerie, L.; Bokobza, L. *Macromolecules* **1982**, *15*, 64.
(37) Itagaki, H.; Horie, K.; Mita, I.; Wasshio, M.; Tagawa, S.; Tabata, Y.; Sato, H.; Tanaka, Y. *Macromolecules* **1987**, *20*, 2774.
(38) (a) Koda, S.; Nomura, H.; Niyahara, Y. *Bull. Chem. Soc. Jpn.* **1979**, *52*, 1828. (b) Froelich, B.; Noel, C.; Jasse, B.; Monnerie, L. *Chem. Phys. Lett.* **1976**, *44*, 159.

Temperature Dependence of Polymer Film Properties on the Air–Water Interface: Poly(vinyl acetate) and Poly(*n*-butyl methacrylate)

Kyung-Hwa Yoo† and Hyuk Yu*

Department of Chemistry, University of Wisconsin, Madison, Wisconsin 53706.
Received July 18, 1988; Revised Manuscript Received March 7, 1989

ABSTRACT: Surface dynamic light scattering is used to deduce the surface viscoelastic properties of poly(vinyl acetate) (PVAc) and poly(*n*-butyl methacrylate) (PnBMA) spread at the air–water interface. The two polymers were selected as group representatives of expanded (PVAc) and condensed (PnBMA) type films. Surface longitudinal viscosity, κ, and elasticity, ϵ, for the two types were calculated from the frequency shift and line broadening of the power spectrum of the scattered light with a dispersion relation over a range of temperatures and surface concentrations. In some cases, the wavevector dependence of the spectral characteristics necessitated the incorporation of a transverse viscosity term, μ, in the dispersion equation, subject to the assumption that ϵ and κ did not depend on the scattering wavevector. This transverse viscosity was shown to have an anomalous temperature dependence with characteristics different for the two polymers; an explanation of the temperature dependence in terms of a slow, collective transverse relaxation process is provided, which may be related to the orientational properties of the different polymers at the interface.

Introduction

Polymer conformation and dynamics at interfaces are important for scientific[1] and technological[2] reasons. It has been known for many years that a wide variety of polymers can be spread at the air–water interface and that measurements of the surface pressure of the resulting films as a function of surface polymer densities suggest grouping polymers according to qualitative differences in their tendency to spread and quantitative differences in their pressure–area curves.[3] For example, poly(vinyl acetate) (PVAc) spreads readily to form fluid (expanded) films stable up to high surface pressures ($\leq$15 dyn cm^{-1}). It is now well established that the reduction in surface tension and the increased damping of surface waves motion, which result when a surface-active film is spread on a liquid surface, are ascribed to the viscoelastic properties of the film. The effects of a surface-active substance on surface waves motion have been examined extensively[4–8] by measuring the attenuation of mechanically excited waves. More recently, the study of the viscoelastic properties of monomolecular films has attracted renewed attention through the introduction of surface light scattering from thermally excited capillary waves since this technique is a noninvasive one. A variety of different materials have been studied by using surface wave scattering.[9–16] On the other hand, very few experiments[12,13] have been directed to probe the temperature dependence of the viscoelastic parameters, which is of major significance since the liquid substrate can be a good or poor "solvent" depending on temperature for a given polymer.[17,18] We present in this report a study of surface light scattering combined with static surface pressure with the use of two polymers,

† Permanent address: Korea Standards Research Institute, Daeduck Danji P.O. Box 3, Daejeon 300-31, Republic of Korea.

0024-9297/89/2222-4019$01.50/0

poly(vinyl acetate) (PVAc) and poly(*n*-butyl methacrylate) (PnBMA), spread at the air–water interface. PVAc and PnBMA have been selected in order to compare the temperature dependence of viscoelasticity between an expanded-type film such as PVAc[3,19] and a condensed-type film such as PnBMA.[3]

In order to describe capillary waves on a film-covered liquid surface, several theoretical models[4,9,20-25] have been developed, which are usually based on the linearized Navier–Stokes equation. They differ mainly in the viscoelastic parameters to be specified. The early theories[4,20] assume that the monolayer is characterized by surface tension and by four other parameters: the dilational and shear elasticities and the dilational and shear viscosities. On the other hand, more recent theories[9,24,25] introduce one more parameter, the transverse viscosity, which originates from the relaxation process of the transverse capillary wave mode of the monolayer. Furthermore, it has been shown[9,25] that, of the dilational and shear elastic and viscous contributions, only the sums of the dilational and shear terms can be resolved. In order to interpret our experimental data, we have chosen the form of the dispersion equation that has four viscoelastic parameters,[20] i.e., the longitudinal elastic modulus and viscosity, and the surface tension, and the transverse viscosity. The shear modes do not couple to fluctuations in the surface film dielectric constants; hence, they cannot be detected by the surface wave scattering technique.[9,24] For the transverse viscosity, it was found[9] that the analysis of the experimental data at a given wavevector k might provide information about whether the transverse viscosity is negligible or not. Our analysis of the results at different wavevectors was aimed at elucidating the temperature dependence of the transverse viscosity, whereby some insight into the mechanism of transverse relaxation processes might be gained and molecular basis of the processes could be inferred.

Experimental Section

Materials. PVAc was prepared by bulk radical polymerization as previously reported in detail.[14] The molecular weight of PVAc was M_v = 114000, which was determined by the intrinsic viscosity in methyl ethyl ketone (MEK) at 25 °C.

PnBMA was obtained from Scientific Polymer Products, Inc. (secondary standards), and purified by dissolving in toluene and precipitating in methanol. The weight- and number-average molecular weights of PnBMA were M_w = 320000 and M_n = 73500, respectively. As the spreading solvent for both polymer films, a spectroscopic grade methylene chloride (Aldrich) was used as received without further purification, since this procedure has been shown to introduce no surface-active impurity.[14]

Methods. The surface pressure and surface wave scattering measurements were performed over the range 15–30 °C for PVAc and 10–25 °C for PnBMA as described in detail elsewhere.[14,26] The substrate temperature was controlled by circulating water kept at constant temperature (±0.1 °C) through a glass coil placed in the bottom of the trough. In order to control the air temperature, a double-walled cabinet enclosing the trough was made of Plexiglas and temperature-controlled air was passed between the walls. In addition, copper tubing coils soldered to a thin copper plate were placed inside the cabinet, and temperature-controlled water was circulated through the copper coils. With these systems, the air temperature was controlled to ±0.1 °C. The surface concentration (Γ) of the polymer film was varied by the sequential addition method as opposed to the compression method.

For the surface light scattering measurement, the spectral shift at the maximum (f_s) and full width at half-height (Δf_s) of the power spectrum were measured. Correction for Δf_s due to instrumental effects was made, following the method of Hård et al.,[27] to give the corrected full width ($\Delta f_{s,c}$). The instrumental corrections to the observed spectral widths amount to 40–60% at low Γ depending on k, as we have documented earlier.[14] Scattering wavevectors, **k**, were slightly different for the two polymers; 260.6, 323.5, and 386.1 cm^{-1} were used for PVAc and 259.7, 321.4, and 382.0 cm^{-1} for PnBMA, corresponding to the spatial wavelength ranges 163–241 and 164–242 μm, respectively.

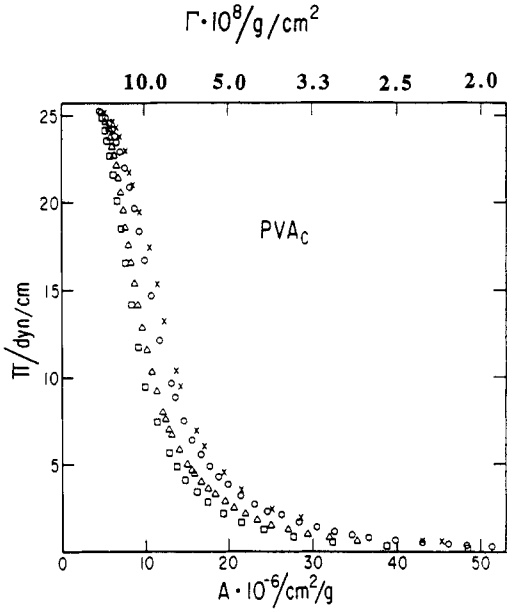

Figure 1. Surface pressure–area (Π–A) isotherms of PVAc film for different temperatures: (×) 30 °C; (○) 25 °C; (△) 20 °C; (□) 15 °C.

Table I
Limiting Areas for PVAc and PnBMA

	A_o, Å²/monomer, at				
	10	15	20	25	30
PVAc	—	17.7	20.9	25.1	27.7
PnBMA	28.4	28.6	31.2	31.5	—

Results and Discussion

PVAc. The surface pressure–area (Π–A) isotherms for PVAc at different temperatures are presented in Figure 1. As the temperature increases at a given surface concentration, $\Gamma = 1/A$, the value of Π increases. The scaling factor υ of $\Pi \sim \Gamma^{\upsilon}$ calculated from the semidilute region of the log Π–log Γ plot for 15 °C was 2.7, which agrees with the literature value.[17] The value of υ remained constant over the temperature range within experimental error. The limiting areas, A_o, obtained by extrapolating to Π = 0 the straight portion of the high-pressure range of Π–A curves, are collected in Table I. The procedure for the extrapolation was detailed elsewhere.[14] The limiting areas of 25.1 Å²/monomer unit for 25 °C and 27.7 Å²/monomer unit for 30 °C are in agreement with those reported by Gabrielli and Puggelli.[28] For the limiting areas at 20 and 15 °C, there are no results available for comparison. The film collapse pressure occurs at about 27.5 dyn/cm, independent of temperature.

Figure 2 shows f_s and $\Delta f_{s,c}$ as a function of Γ at 20 and 25 °C at three different k values. Up to $\Gamma = 4 \times 10^{-8}$ g/cm², the differences between the values of f_s at 25 °C and those at 20 °C are almost the same as those found for the free water surface. In the region $\Gamma = 4 \times 10^{-8}$–$15 \times 10^{-8}$ g/cm², the temperature dependence emerges beyond that of the pure substrate, and above this region, the values of f_s at 20 °C are almost equal to those at 25 °C.

In the $\Delta f_{s,c}$–Γ plot, two maxima and one minimum are noted for both 20 and 25 °C. The first peak positions are at $\Gamma = 5.7 \times 10^{-8}$ g/cm² at 25 °C and $\Gamma = 6.7 \times 10^{-8}$ g/cm² at 20 °C, which correspond quite closely to the limiting surface concentrations ($\Gamma_o = 1/A_o$). This implies that the

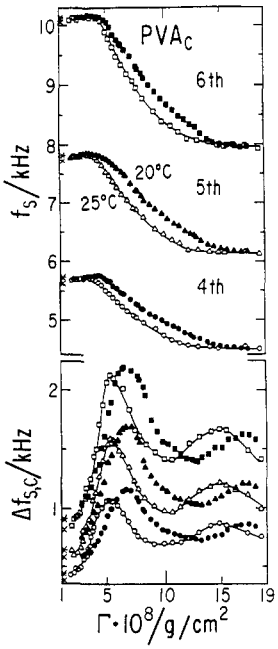

Figure 2. Peak frequency (f_s) and corrected full width ($\Delta f_{s,c}$) as a function of surface concentration for PVAc at 20 and 25 °C. (○) Fourth order, k = 260.6 cm^{-1}; (△) fifth order, k = 323.5 cm^{-1}; (□) sixth order, k = 386.1 cm^{-1} for 25 °C. The filled circles, triangles, and squares correspond to data for 20 °C. (×) f_s and $\Delta f_{s,c}$ of free substrate for 25 °C; (*) f_s and $\Delta f_{s,c}$ of the free substrate for 20 °C. The solid curves are drawn to indicate the average trends at 25 °C.

wave damping is at a maximum when the monolayer is closely packed. The minimum and second maximum positions of $\Gamma = 13 \times 10^{-8}$ and 17×10^{-8} g/cm^2 at 20 °C are shifted to smaller values of $\Gamma = 10.5 \times 10^{-8}$ and 15×10^{-8} g/cm^2 at 25 °C; these shifts are larger amounts than the first peakshift relative to temperature. A similar dependence was observed at 15 and 30 °C.

The surface light scattering results were analyzed to obtain film viscoelastic parameters using the following dispersion relation:[22]

$$\left[\eta(k+m) - \frac{\epsilon^* k^2}{i\omega}\right]\left[\frac{\eta m(k+m)}{k} - \frac{\sigma^* k^2}{i\omega}\right] = \eta^2(k-m)^2 \tag{1}$$

where

$$\epsilon^* = \epsilon - i\omega\kappa, \qquad m = \left[k^2 - \frac{i\omega\rho}{\eta}\right]^{1/2},$$
$$\sigma^* = \sigma_d - i\omega\mu, \qquad \omega = 2\pi f_s - 2\pi i(\Delta f_{s,c}/2)$$

ϵ is the film longitudinal elasticity which is the sum of the dilational and shear components, κ is the corresponding viscosity which is also the sum of the dilation and shear viscosities, ρ is the bulk density of the substrate, η is the shear viscosity of the substrate, σ_d is the dynamic surface tension, and μ is the film transverse viscosity. We should note here that this analysis gives no unique determination of viscoelastic parameters even when viscoelastic parameters are independent of ω, since four viscoelastic parameters (i.e., ϵ, κ, σ_d, and μ) have to be extracted from two experimental values (i.e., f_s and $\Delta f_{s,c}$) at a given value of k. Thus, several assumptions concerning viscoelasticity are required to interpret experimental data. Initially, we assumed that σ_d was equal to the static surface tension (σ_s) as measured by the Wihelmy plate technique, μ was negligible, and the parameters, ϵ and κ, were independent of ω. Once ϵ and κ are calculated with these assumptions from f_s and $\Delta f_{s,c}$ at different k values and they turn out to be independent of k, the assumptions can then be considered reasonable. On the other hand, if ϵ and κ so calculated do depend on k, then it may be that (1) the relaxation effect of the vertical motions of the film is not negligible, i.e., $\mu \neq 0$, or (2) ϵ and κ are not independent of ω,[21] or (3) both may be true. If viscoelastic parameters depend on ω, ϵ^* and/or σ^* becomes so complicated that it is almost impossible to interpret data quantitatively. Hence, where ϵ and κ obtained with the above assumptions were found to be dependent on k, quantitative analysis regarding the frequency dependence of viscoelasticity was not attempted, primarily because our range of available k is so small that full examinations of k dependence at this point are rather unproductive; in such cases, only the transverse motion will be considered.

We should thus note that the parameters we deduce, σ_d, ϵ, κ, and μ, are still subject to the assumptions that (i) $\sigma_d \geq \sigma_s$, (ii) $\mu \geq 0$, and (iii) σ_d and ϵ should be frequency independent. To this extent, the parameters we report here are model dependent and only ranges can be specified, hence not to be taken as definitive. It is far more plausible to assume that $\epsilon^* = \epsilon^*(\omega)$ and $\sigma^* = \sigma^*(\omega)$, whereby all four parameters, ϵ, κ, σ_d, and μ, are frequency dependent. Unfortunately, we cannot start with this assumption and hope to interpret the results for two experimental quantities, f_s and $\Delta f_{s,c}$, having the predicted k dependences. This is a crucial caveat we offer to the reader before proceeding further with the analysis of results.

The dependences of calculated ϵ and κ on surface concentration at 20 °C for three different k values are shown in parts A and B of Figure 3, respectively. No k dependence of ϵ and κ was found, within experimental error. The dotted curve in Figure 3A represents the static elasticity (ϵ_s) calculated from the Π–A plot in Figure 1 with the commonly used relation

$$\epsilon_s = -A(\partial\Pi/\partial A)_T \tag{2}$$

Both ϵ and ϵ_s have their maximum values at $\Gamma \simeq 12 \times 10^{-8}$ g/cm^2, although the magnitude of ϵ is larger than that of ϵ_s in the vicinity of maximum.

In the plot of κ versus Γ (Figure 3B), we see that the value of κ is negligible up to $\Gamma \simeq 3 \times 10^{-8}$ g/cm^2. In the region of $\Gamma = 3 \times 10^{-8}$–$6.7 \times 10^{-8}$ g/cm^2, a small maximum is observed. Similar observations have been made earlier[14,16] for this feature in the κ–Γ plot for PVAc at 25 °C. From $\Gamma = 6.7 \times 10^{-8}$ to 13×10^{-8} g/cm^2, corresponding to the first maximum and minimum positons of $\Delta f_{s,c}$ respectively, the value of κ increases and then decreases. Above $\Gamma = 15 \times 10^{-8}$ g/cm^2, it is estimated[14] that the polymer film might no longer be a monolayer; hence eq 1 might not be applicable, so ϵ and κ are not calculated. From the behavior of κ versus Γ, it was inferred that the surface concentration range can be divided into five regimes, the conformational state of the film being different in each region. Indeed, based on the surface wave scattering measurements of PVAc film at 25 °C, a tentative model of the conformation states was proposed by Kawaguchi et al.[14] to account for the existence of these five regimes. They are recalled as follows: (1) dilute solution with isolated two-dimensional chains; (2) semidilute and intermediate concentration, with close-packed two-dimensional chains giving rise to monolayers at the end of this regime; (3) dynamic chain looping state where polymer molecules start to have short loops off the substrate surface because of insufficient adsorption sites per molecule; (4) loop thickening regime at the end of which the average loop size comes to a saturation limit, giving rise to the chain loops monolayer state; and (5) chain pileup over those

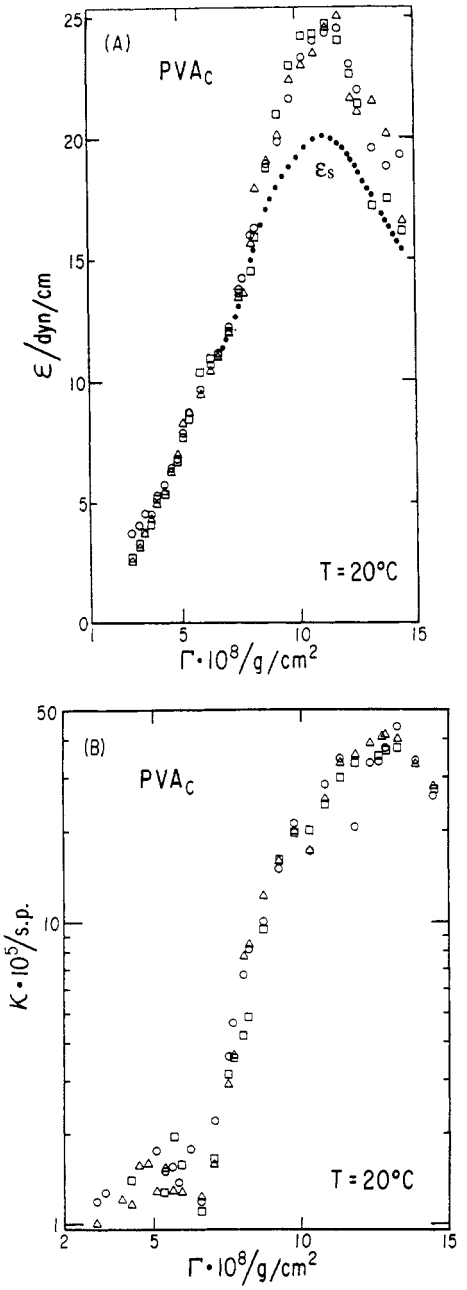

Figure 3. Calculated ϵ (A) and κ (B) as a function of surface concentration for PVAc at 20 °C. (○) k = 260.6 cm^{-1}; (△) k = 323.5 cm^{-1}; (□) k = 386.1 cm^{-1}. The dotted curve in A represents the static elasticity (ϵ_s).

partially adsorbed with the loops. The data we present in Figure 3 are in agreement with the results of Kawaguchi et al.[14,16] at the same temperature of 25 °C.

In Figure 4, A and B, the ϵ and κ calculated assuming that $\sigma_d = \sigma_s$ and $\mu = 0$ and by using eq 1 at 25 °C are given as a function of surface concentration at three different k values. Unlike the case at 20 °C, ϵ and κ are indeed different for different k values above $\Gamma = 5.7 \times 10^{-8}$ g/cm^2, indicated by an arrow. Furthermore, anomaly of ϵ decreasing with increasing k is obvious; this appears to indicate that elasticity decreases with increasing frequency, contrary to any viscoelastic behaviors. We thus start with the postulate that this k dependence is due to the transverse contribution, i.e., $\mu \neq 0$, rather than frequency dependence of ϵ and κ; it appears plausible for two reasons. Firstly, k dependence begins to appear in the region of the closely packed state, where it could begin to be sensitive to the relaxation processes of the vertical motion. Secondly, according to Mann and Du,[21] the effect of frequency

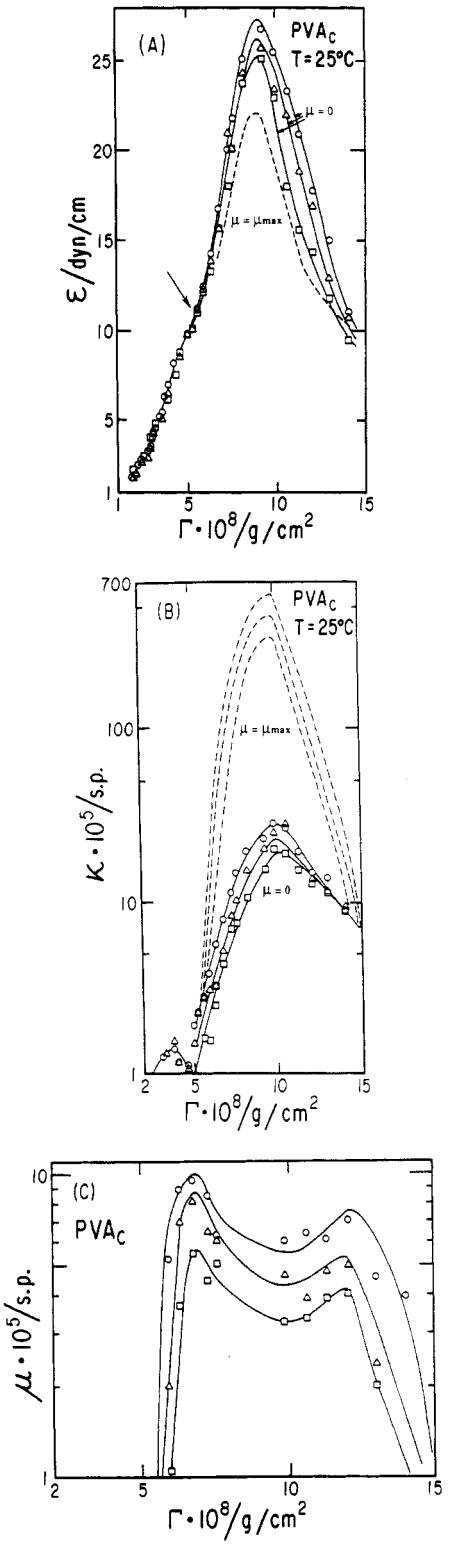

Figure 4. Calculated ϵ (A), κ (B), and μ (C) as a function of surface concentration for PVAc at 25 °C. (○) k = 260.6 cm^{-1}; (△) k = 323.5 cm^{-1}; (□) k = 386.1 cm^{-1}. The solid curves in A and B were calculated from the solid curves in Figure 2, neglecting the transverse viscosity, $\mu = 0$. The solid curve in C shows the maximum value of μ obtained from the solid curves in Figure 2. The broken curves in A and B represent the ϵ and κ values calculated using the solid curve in C. See text for details.

dependence of the viscosity coefficients is more significant in the lower surface pressure region than in the higher surface pressure region. We therefore tried to search for values of μ and σ_d that would render ϵ and κ independent of k. Thus, with the assumptions that $\sigma_d \geq \sigma_s$ and that $\mu \geq 0$, we solve for eq 1 analytically to find the maximum

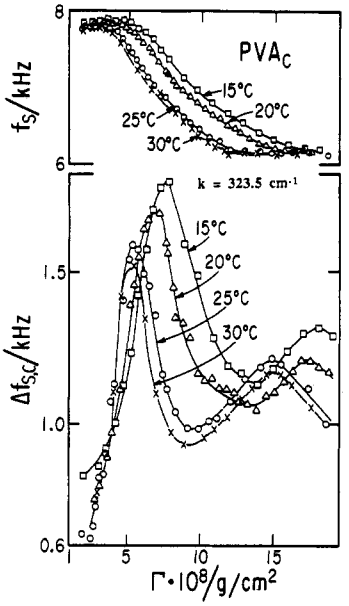

Figure 5. f_s and $\Delta f_{s,c}$ as a function of surface concentration for PVAc at k = 323.5 cm^{-1}: (×) 30 °C; (○) 25 °C; (△) 20 °C; (□) 15 °C. The solid curves are drawn over the data points to indicate the average trends.

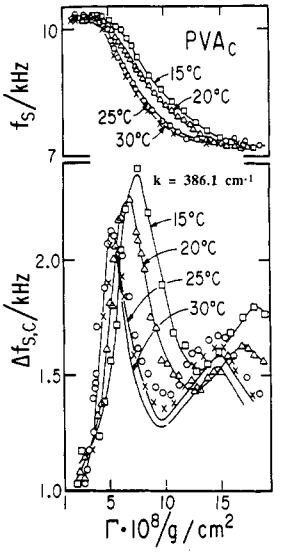

Figure 6. f_s and $\Delta f_{s,c}$ as a function of surface concentration for PVAc at k = 386.1 cm^{-1}: (×) 30 °C; (○) 25 °C; (△) 20 °C; (□) 15 °C. The solid curves represent f_s and $\Delta f_{s,c}$ calculated using the ϵ and κ values obtained from the solid curves in Figure 5, neglecting the transverse viscosity, μ = 0. See text for details.

and minimum values of the four viscoelastic parameters which are all consistent with the input experimental quantities, f_s and $\Delta f_{s,c}$. It was found that σ_d was equal to σ_s up to $\Gamma = 15 \times 10^{-8}$ g/cm^2. The minimum value of μ is zero, and the maximum values of μ are presented in Figure 4C. The broken curves in Figure 4, A and B, represent the values of ϵ and κ calculated using the maximum value of μ. The effect of increasing μ from zero to make ϵ decrease and κ increase. It is clear from Figure 4A that k dependence of ϵ at $\mu = 0$ disappears at $\mu = \mu_{max}$ and the magnitude of ϵ is not greatly changed. On the other hand, Figure 4B shows that κ increases by over an order of magnitude and its k dependence is further amplified as μ is allowed to be nonzero and reaches its maximum possible values. Figure 4C shows that μ_{max} is also k dependent. Thus, we conclude in this instance that the criterion of k independence for the viscoelastic parameters would appear insufficient to determine whether $\mu = 0$ or $\mu > 0$, and our attempt here seems to be a mixed success. In the dilute concentration region where ϵ and κ are independent of k, the value at 25 °C is smaller than that at 20 °C, which is expected for viscosity.

The effect of decreasing ϵ and increasing κ with increasing μ is not physically obvious, and we do not fully understand these trends. Nevertheless, it is tempting to suggest that the coupling of the transverse mode with its relaxation effect, i.e., $\mu > 0$, with the longitudinal mode with both of its components, ϵ and κ, requires an adjustment of ϵ and κ to conserve the capillary wave propagation rate (f_s) and its temporal damping ($\Delta f_{s,c}$). A simpler explanation may be that an increase in the transverse wave viscous component must result in an increase in the longitudinal wave viscous component by virtue of the mode coupling, and its consequence is to reduce ϵ as long as σ_d is held constant, since σ_d is principally responsible for f_s and ϵ, κ, and μ must adjust to produce the same $\Delta f_{s,c}$ value.

Comparing our results for 20 °C with those at the same temperature previously reported by Langevin,[9] who calculated viscoelastic parameters using the profile of power spectrum for the capillary wave instead of just extracting f_s and $\Delta f_{s,c}$ from the power spectrum and using eq 1 to deduce σ_d, ϵ, κ, and μ under a set of assumptions as we have done here, we find some differences. Langevin suggested that μ was not negligible and that σ_d was larger than σ_s in some regions at 20 °C, whereas we find that the transverse relaxation was negligible in all surface concentrations at 20 °C. Therefore, we considered the possibility that this discrepancy might be due to the different analysis procedures used. In order to test this hypothesis, the values of ϵ and κ obtained by using eq 1 from f_s to $\Delta f_{s,c}$ for k = 323.5 cm^{-1}, as represented by the solid curves in Figure 5, were used to compute f_s and $\Delta f_{s,c}$ for another wavevector, k = 386.1 cm^{-1}, using eq 1, and these were compared to those calculated from the profile of power spectrum given by[9,29]

$$P_z(\omega) = -(k_\beta T/\pi\omega)(\tau_0{}^2 k/\rho)\ \mathrm{Im}\ [\{S^2 + (\alpha y + \beta S) \times [(1 + 2S)^{1/2} - 1]\} D^{-1}(S)] \quad (3)$$

where

$$y = \sigma_d \rho/4\eta^2 k, \qquad \tau_0 = \rho/2\eta k^2, \qquad S = i\omega\tau_0,$$
$$\alpha = \epsilon/\sigma_d, \qquad \beta = \kappa k/2\eta, \qquad \gamma = \mu k/2\eta,$$

$$D(S) = S^2[(1 + S)^2 + y - (1 + 2S)^{1/2}] + (\alpha y + \beta S) \times [S^2(1 + 2S)^{1/2} + (y + \gamma S)\{(1 + 2S)^{1/2} - 1\}] + \gamma S^3$$

and k_B is the Boltzmann constant. In the calculations, $\sigma_d = \sigma_s$ and $\mu = 0$ were assumed. Values of f_s and $\Delta f_{s,c}$ obtained by solving eq 3 were the same as those calculated from eq 1 to within 1% in our range of k values available. This suggests that the discrepancy between Langevin's results and our results comes from factors other than the different analysis schemes. As alternative explanations for the discrepancy, the different correction methods[27,29] for the instrumental width and the large error involved in determining viscoelastic parameters, particularly so when only one k value is used in the measurement, as Langevin has done, may be mentioned. At any rate, the two different analysis schemes yield the same results, whereby our present analysis scheme may be taken to be as good as that of solving for eq 3.

Figure 5 shows f_s and $\Delta f_{s,c}$ for one wavevector (k = 323.5 cm^{-1}) and all four temperatures. The data points have been fitted with smooth curves for ready comparisons among the data at different temperatures. We first assumed that μ was zero for all wavevectors. Solid curves in Figure 6 represent f_s and $\Delta f_{s,c}$ calculated at k = 386.1 cm^{-1} using the data in Figure 5 at all temperatures. It is

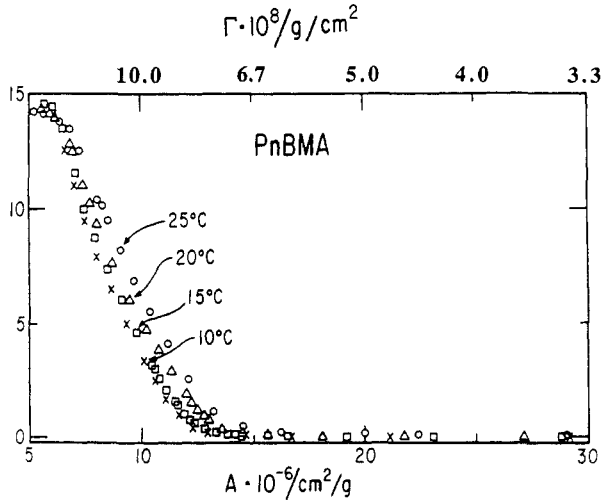

Figure 7. Π–*A* isotherms of PnBMA film for different temperatures: (○) 25 °C; (△) 20 °C; (□) 15 °C; (×) 10 °C.

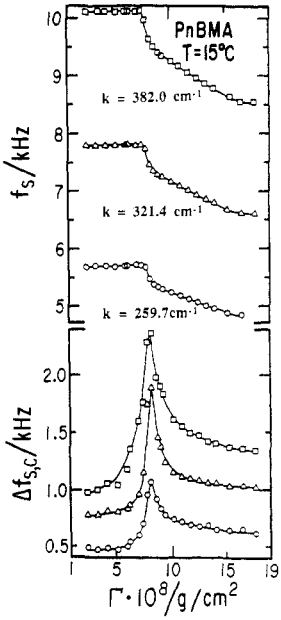

Figure 8. f_s and $\Delta f_{s,c}$ as a function of surface concentration for PnBMA at 15 °C. (○) k = 259.7 cm^{-1}; (△) k = 321.4 cm^{-1}; (□) 382.0 cm^{-1}.

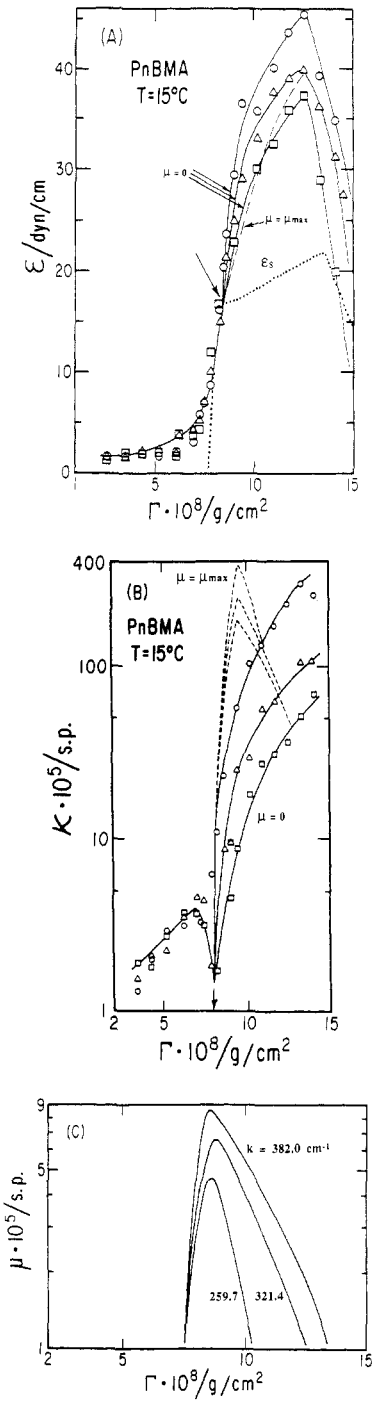

Figure 9. Calculated ϵ (A), κ (B), and μ (C) as a function of surface concentration for PnBMA at 15 °C. (○) k = 259.7 cm^{-1}; (△) k = 321.5 cm^{-1}; (□) k = 382.0 cm^{-1}. The dotted curve in A shows ϵ_s. The solid curves in A and B were calculated from the solid curves in Figure 8, neglecting the transverse viscosity. The curves in C show the maximum values of μ obtained from the solid curves in Figure 8 with sixth order, k = 382.0 cm^{-1}; fifth order, k = 321.5 cm^{-1}; and fourth order, k = 259.7 cm^{-1}. The broken curves in A and B represent the ϵ and κ values calculated using the solid curve in C. See text for details.

apparent that the solid curves are in accord with the measured values at 15 and 20 °C whereas at 25 and 30 °C differences between the calculated and measured values emerge after the first maximum position of $\Delta f_{s,c}$. This could be taken as an indication that for 25 and 30 °C the transverse viscosity of the PVAc film may not be zero, provided the observed k dependence is at least partly due to the transverse relaxation, while for 15 and 20 °C the transverse viscosity is unobservable. This kind of temperature dependence of μ has also been reported by Crawford and Earnshaw,[13] who performed experiments with the solvent-free monoglyceride bilayer membrane using the same surface light scattering technique.

PnBMA. Figure 7 shows curves of Π versus A for PnBMA at four different temperatures. For A greater than 15 × 10^6 cm^2/g, Π is almost zero at all temperatures. Below this value of A, the Π–A curve begins to increase rather steeply with decreasing A; such a behavior is characteristic of the Π–A isotherm of the condensed-type film.[3] The exponent υ of Π ~ Γ^{υ} calculated from the semidilute region of the log Π–log Γ plot (not shown) for 15 °C was 13, corresponding to the value for poor solvent conditions,[17,18] and υ was not sensitive to temperature over the range 10–25 °C. The limiting areas per monomer, A_o, are collected in Table I. The values are in agreement with those in the literature.[3]

Values of f_s and $\Delta f_{s,c}$ at 15 °C at three different k values as a function of the surface concentration are plotted in Figure 8. Up to Γ = 7 × 10^{-8} g/cm^2, f_s is nearly constant for each k value. With increasing Γ, a very slight increase in f_s is followed by an abrupt decrease. In the case of $\Delta f_{s,c}$,

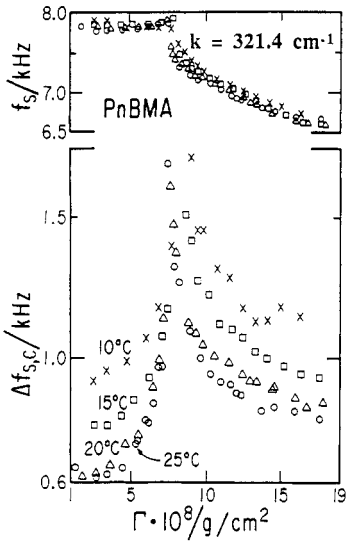

Figure 10. f_s and $\Delta f_{s,c}$ as a function of surface concentration of PnBMA at k = 321.4 cm^{-1}: (○) 25 °C; (△) 20 °C; (□) 15 °C; (×) 10 °C.

it increases gradually with Γ in the dilute region, where f_s and Π do not change substantially. At around Γ = 8 × 10^{-8} g/cm^2, where f_s drops rapidly, $\Delta f_{s,c}$ steeply increases and then precipitously decreases. This kind of sharp increase of $\Delta f_{s,c}$ also has been found in poly(methyl methacrylate), but in this case, a much more gradual decrease followed.[30]

Analysis schemes for PnBMA are the same as for PVAc. In Figure 9, A and B, ϵ and κ at 15 °C, calculated from eq 1 neglecting the transverse viscosity, μ = 0, are plotted against Γ for each k value. Below Γ = 8 × 10^{-8} g/cm^2, the values of ϵ and κ are almost the same for all k values. However, above this value of Γ, that k dependence of ϵ and κ appears, and the similar anomaly of k dependence on ϵ appears as PVAc at 25 °C, which is taken as an indication that the transverse viscosity may not be ignored. Thus, with the same method as for PVAc at 25 °C, the maximum and minimum values of the viscoelastic parameters were calculated, and σ_d was found to be equal to σ_s for all surface concentrations. The maximum possible value of μ is presented in Figure 9C. The broken curves in Figure 9, A and B, represent ϵ and κ calculated from eq 1 with the maximum value of μ. As for PVAc, when μ is increased from zero to μ_{max}, ϵ is decreased and κ increased relative to their values for μ = 0. The values of ϵ and κ obtained assuming $\sigma_d = \sigma_s$ and μ = 0 at 10, 20, and 25 °C were also found to be dependent on k at Γ greater than the one (8 × 10^{-8} g/cm^2) corresponding to the peak in $\Delta f_{s,c}$.

In order to display the temperature dependence of the film properties, plots of f_s and $\Delta f_{s,c}$ versus Γ for all temperatures at k = 321.4 cm^{-1} are presented in Figure 10. As with PVAc, the maximum positions of $\Delta f_{s,c}$ for all temperatures are consistent with the value for A_0. The solid curves in Figure 11, A and B, represent values of ϵ and κ calculated by using eq 1 assuming $\sigma_d = \sigma_s$ and μ = 0. Up to Γ_0 (i.e., $1/A_0$), where we suggest that the transverse viscosity may be negligible, κ increases as the temperature is decreased, while ϵ remains insensitive to temperature. Beyond Γ_0, the maximum and minimum values of viscoelastic parameters were calculated with $\mu > 0$. For all temperatures, it was found that σ_d was equal to σ_s. The maximum possible values of μ consistent with the data are given in Figure 11C, and the values of ϵ and κ assuming the maximum value of μ are represented by the broken curves in Figure 11, A and B. As the temperature rises, the maximum values of κ and μ decrease, whereas both minimum and maximum values of ϵ increase.

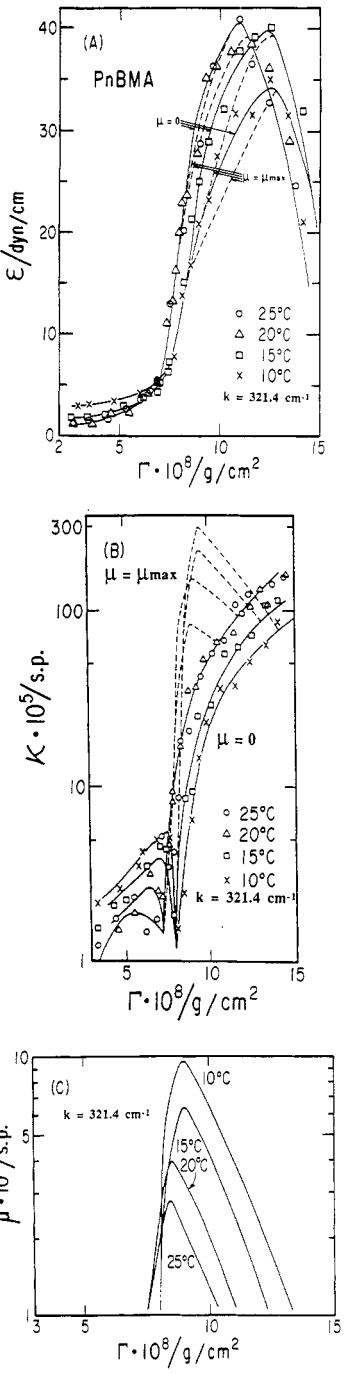

Figure 11. Calculated ϵ (A), κ (B), and μ (C) as a function of surface concentration for PnBMA at k = 321.4 cm^{-1}. The solid curves in A and B were calculated from the smoothed curves over the data points of f_s and $\Delta f_{s,c}$ in Figure 10 (not shown for clarity), neglecting the transverse viscosity, μ = 0. The solid curve in C shows the maximum values of μ obtained from the smoothed curves over the data points of f_s and $\Delta f_{s,c}$ in Figure 10. The broken curves in A and B represent the ϵ and κ values calculated with the solid curve in C. See text for details.

In terms of μ, the PVAc and PnBMA films show quite different temperature dependences. As the temperature decreases, the maximum possible μ value, consistent with our data, for PVAc becomes negligible, while that for PnBMA increases. This contrast in the temperature dependence seems anomalous, though we emphasize that the maximum possible value of μ may not be real; thus, the interpretation is subject to the caveat we offered earlier. Langevin[9] has reported an anomalous dependence of μ on Γ; μ was observed to increase with increasing concentration up to a limiting concentration above which μ fell to zero.

Langevin offered an interpretation of this result in terms of a limiting slow relaxation process associated with the transverse viscosity. Our temperature dependence may be similarly explained. Thus, μ depends on frequency and, for example, has a frequency dependence of the form proposed by Mann and Du,[21]

$$\mu = \mu^{\infty} + [\tau\theta/(1 - i\omega\tau)] \quad (4)$$

where τ is the relaxation time, θ is the scaling constant of the non-Newtonian response of the system, and μ^{∞} is the high-frequency limiting viscosity which may be assumed to be zero. According to eq 4, the imaginary part of μ has a maximum value when $\omega\tau = 1$ (i.e., $\tau = 1/\omega$). Thus, since the relaxation time, τ, is expected to become longer as the temperature is decreased, if $\omega\tau < 1$ in the temperature range of interest, μ increases as the temperature decreases; if $\omega\tau > 1$, μ decreases with decreasing temperature. It follows that, if the predominant relaxation time of PVAc is greater than $1/\omega$ and if of PnBMA is less than $1/\omega$, different temperature dependences of μ would be observed. To our knowledge, there is no experimental data to support or test this assumption about the relaxation time. However, since it has been suggested that PVAc is horizontally oriented[19,31] and PnBMA is more nearly vertically oriented,[19] it may follow that the relaxation time, τ, associated with the transverse motion of PVAc is longer than that of PnBMA.

In summary, studies of this sort to probe the transverse viscosity contribution to film viscoelasticity might well bring forth new insight into the chain conformational dynamics at the air-water interface. With the present study, we would suggest that the relaxation processes associated with transverse motions may be of significance in defining the interfacial conformational dynamics; at least we cannot outright ignore it under all circumstances.

Acknowledgment. This work was in part supported by the Miami Valley Laboratories of the Procter and Gamble Company and the Research Committee of the University of Wisconsin—Madison. Additional support by the Research Laboratories of Eastman Kodak Company is gratefully acknowledged.

Registry No. PVAc, 9003-20-7; PnBMA, 9003-63-8.

References and Notes

(1) de Gennes, P.-G. *Adv. Colloid Interface Sci.* **1987**, *27*, 189.
(2) Wu, S. *Polymer Interface and Adhesion*; Marcel Dekker: New York, 1982.
(3) Crisp, F. J. *J. Colloid Sci.* **1946**, *1*, 49, 161.
(4) Goodrich, F. C. *Proc. R. Soc. London* **1961**, *A260*, 490, 503.
(5) Davies, J. T.; Vose, R. W. *Proc. R. Soc. London* **1965**, *A286*, 218.
(6) Lucassen, J.; Hansen, R. S. *J. Colloid Interface Sci.* **1966**, *22*, 32; **1967**, *23*, 319.
(7) Bendure, R. L.; Hansen, R. S. *J. Phys. Chem.* **1967**, *71*, 2889.
(8) Thiessen, D.; Scheludko, A. *Kolloid-Z., Polym.* **1967**, *218*, 139.
(9) Langevin, D. *J. Colloid Interface Sci.* **1981**, *80*, 412.
(10) Hård, S.; Löfgren, H. *J. Colloid Interface Sci.* **1977**, *60*, 529.
(11) Hård, S.; Neuman, R. D. *J. Colloid Interface Sci.* **1981**, *83*, 315.
(12) Crilly, J. F.; Earnshaw, J. C. In *Biomedical Applications of Laser-Light Scattering*; Sattelle, D. B., Lee, W. I., Ware, B. R., Eds.; Elsevier: Amsterdam, 1982.
(13) Crawford, G. E.; Earnshaw, J. C. *Biophys. J.* **1986**, *49*, 869.
(14) Kawaguchi, M.; Sano, M.; Chen, Y.-L.; Zografi, G.; Yu, H. *Macromolecules* **1986**, *19*, 2606.
(15) Chen, Y.-L.; Kawaguchi, M.; Yu, H.; Zografi, G. *Langmuir* **1987**, *3*, 31.
(16) Sauer, B. B.; Kawaguchi, M.; Yu, H. *Macromolecules* **1987**, *20*, 2732.
(17) Vilanove, R.; Rondelez, F. *Phys. Rev. Lett.* **1980**, *45*, 1502.
(18) Takahashi, A.; Yoshida, A.; Kawaguchi, M. *Macromolecules* **1982**, *16*, 1196.
(19) Pak, H.; Kawaguchi, M.; Sano, M.; Yoo, K.-H.; Yu, H. *Macromolecules*, submitted.
(20) Lucassen-Reynders, E. H.; Lucassen, J. *Adv. Colloid Interface Sci.* **1969**, *2*, 347.
(21) Mann, J. A.; Du, G. *J. Colloid Interface Sci.* **1971**, *37*, 2.
(22) Kramer, L. *J. Chem. Phys.* **1971**, *55*, 2097.
(23) Goodrich, F. C. *J. Phys. Chem.* **1962**, *66*, 1858.
(24) Langevin, D.; Griesman, C. *J. Phys. D* **1980**, *13*, 1189.
(25) Mann, J. A., Jr. In *Surface and Colloid Science*; Matijevic, E., Robert, J. G., Eds.; Plenum: New York, 1984; Vol. 13.
(26) Sano, M.; Kawaguchi, M.; Chen, Y.-L.; Skarlupka, R. J.; Chang, T.; Zografi, G.; Yu, H. *Rev. Sci. Instrum.* **1986**, *57*, 1158.
(27) Hård, S.; Hamnerius, Y.; Nilsson, O. *J. Appl. Phys.* **1976**, *47*, 2433.
(28) Gabrielli, G.; Puggelli, M. *Colloid Interface Sci.* **1971**, *35*, 460.
(29) Langevin, D. *J. Chem. Soc., Faraday Trans. 1* **1974**, *70*, 95.
(30) Kawaguchi, M.; Sauer, B. B.; Yu, H. *Macromolecules* **1989**, *22*, 1735.
(31) Ries, H. E., Jr.; Walker, D. C. *J. Colloid Sci.* **1961**, *16*, 361.

Influence of the Acid Residue on the Polarity of Cycloaliphatic Polyesters

Evaristo Riande,* Julio Guzmán, and Javier de Abajo

Instituto de Ciencia y Tecnología de Polímeros, 28006-Madrid, Spain.
Received December 8, 1988; Revised Manuscript Received March 4, 1989

ABSTRACT: The cis and trans isomers poly(1,4-cyclohexanedimethanol adipate) (PCCDA and PTCDA) and poly(*trans*-1,4-cyclohexanedimethanol succinate) (PTCDS) were synthesized by condensation of the corresponding cis and trans isomers of 1,4-cyclohexanedimethanol with adipic acid and succinic acid, respectively. The values of the dipole moment ratio $\langle\mu^2\rangle/nm^2$ at 30 °C for PCCDA, measured in benzene and dioxane solutions, were found to be 0.950 and 0.914, respectively. The values of the dipole moment ratio of PTCDA and PTCDS, determined from dielectric constant measurements in dilute dioxane solutions at 50 and 70 °C, were 0.596 and 0.454, respectively. In general, the trans isomers exhibit lower polarity than the cis, and the values of the dipole moment ratio of the former polyesters seem to decrease as the number of methylene groups in the acid residue decreases. The trans isomers also exhibit a positive and larger temperature coefficient than the cis isomers. Theoretical calculations carried out with the rotational isomeric state model give a good account of the experimental results, assuming that gauche states about CH_2–CO bonds of the acid residue are preferred over the alternative trans states. The theoretical analysis also suggests that the trans states about the β CH_2–CH_2 bonds of the acid residue are preferred over the corresponding gauche states.

Introduction

Polyesters and polyformals obtained by reaction of cyclohexanedimethanol with aliphatic acids and formaldehyde, respectively, were recently studied with the aim of analyzing the influence of the substitution (equatorial–axial or equatorial–equatorial) of the hydrogen atoms

0024-9297/89/2222-4026$01.50/0